PALEOBIOLOGY
A PUBLICATION OF THE
Paleontological
S O C I E T Y

Article

The effect of siliceous sponge deposition on Permian paleocommunity structure

Zackery P. Wistort* and *Kathleen A. Ritterbush*

Abstract.—A dramatic shift from carbonate-rich to chert-rich marine strata occurred during the Permian and is frequently attributed to the increased activity of siliceous sponges and their biosiliceous sedimentation. The first-order ecologic consequences of this transition, if any, remain opaque. We analyze fossil occurrence data from the Phosphoria Basin (western North America) to test whether the presence of siliceous sponges, which are correlated with basin-wide chert strata, influenced the recruitment of benthic fauna. Using published lithologic descriptions, we categorized fossil collections by formation, facies, and lithology and used these data to code detrended correspondence analysis and nonmetric multidimensional scaling ordinations. We also analyzed the clustering of taxa into faunal units termed biofacies.

   Results from these analyses indicate that fossil collections occurring in chert and carbonate are closely associated in faunal composition and community structure. These collections preferentially occur in the inner- to mid-ramp facies, in agreement with previous studies. Although largely similar in composition, collections of chert and carbonate lithology exhibit differences in the frequency and abundance of accessory brachiopod taxa (e.g., *Composita* and *Hustedia*), possibly a result of greater biosiliceous sedimentary input.

Zackery P. Wistort[†] and Kathleen A. Ritterbush. Department of Geology and Geophysics, University of Utah, Salt Lake City, Utah 84112, U.S.A. E-mail: zwistort@fau.edu. [†]Present address: Harbor Branch Oceanographic Institute, Florida Atlantic University, Fort Pierce, Florida 34946, U.S.A. E-mail: k.ritterbush@utah.edu.

Introduction

Chert forms through recrystallization of unstable variants of quartz, which can accumulate from inorganic or organic deposition (e.g., volcanic ash and eolian silicates vs. diatoms, radiolarians, and siliceous sponges). Chert strata are prominent in the epicratonic basins that lined the northwestern coast of Pangea during the Permian. From southernmost to northernmost, these include the Permian Basin (western Texas, USA); Phosphoria Basin (western United States); Ishbel Group (western Canada); Sverdrup Basin (Arctic Canada); and Kapp Starostin Formation (Svalbard, Norway) (Murchey and Jones 1992; Beauchamp and Baud 2002; Piper and Link 2002; Hiatt and Budd 2003; Gates et al. 2004; Ketner 2009; Ritterbush 2019). The widespread occurrence of abundant, contemporaneous cherty strata is dubbed the "Permian chert event" (Murchey and Jones 1992; Beauchamp and Baud 2002).

Changing environmental conditions are credited with the region's switch from carbonate-rich to biosiliceous-rich sedimentation. In general, the Permian chert event is interpreted as a transition from a predominantly warm-water and photozoan-dominant carbonate ramp system to a cool-water and heterozoan-dominant carbonate ramp/glass ramp system (à la Gates et al. 2004). A glass ramp is a depositional system in which biosiliceous skeletal elements are a primary contributor to sediment deposition. Cooling of regional Panthalassic circulation is attributed to a shift in the prevailing ocean currents, as an occlusal of the Uralian Seaway may have prevented cool boreal to polar currents from

returning to the warm Paleo-Tethys Sea (Zharkov and Chumakov 2001; Beauchamp and Baud 2002; Blakey 2003; Reid et al. 2007). Along the northwestern flank of Pangea, this circulation change may have fomented a thermohaline circulation regime that drove cold, nutrient-rich waters down the western coast. The initiation of seasonally driven coastal upwelling is widely inferred (Beauchamp and Baud 2002; Piper and Link 2002; Hiatt and Budd 2003; Reid et al. 2007; Clapham 2010; Beauchamp and Grasby 2012; Schoepfer et al. 2012, 2013), but faces unresolved paleogeographic objections (Ketner 2009; see discussion in Ritterbush 2019). Overall, broad environmental changes are credited with wholesale biotic reorganization during this time, including expansion of the sponges, but internal fauna-to-fauna interactions remain underexplored.

Here, we explore what role, if any, the siliceous sponges played in reorganizing benthic paleoecologic community structure during the Permian chert event. To assess this question, we digitized fossil occurrences and lithologic data from across the Phosphoria Basin as compiled by Yochelson and Van Sickle (1968). This record offers two distinct advantages. First, these published data cover a broad spatiotemporal range with ample fossil collections and detailed lithologic information for the Phosphoria Basin's primary depositional cycles (e.g., Franson, Ervay). Second, while modern siliceous sponges remain critical in benthic ecosystems worldwide, these ancient examples recorded much larger, longer, and more intense sponge expansions than any shallow or coastal setting today (Beauchamp and Baud 2002; Gates et al. 2004; Murchey 2004; Ritterbush 2019).

Although the Phosphoria Basin has been extensively sampled, sponge body fossils are reported from only a few localities (*Actinocoelia maeandrina* [Finks et al. 1961]; *Haplistion* sp. [Yochelson and Van Sickle 1968]; *Virgaspongiella ramosa* and *Incrustatospongia superficiala* [Rigby and Boyd 2004]). In general, sponges are primarily composed of soft tissues (spongin) and thus are unlikely to preserve as singular occurrences. Upon demise, the spongin holding a sponge together degrades and the micron-scale, skeletal elements of the sponge

(spicules) disarticulate. This is problematic when trying to untangle the relationship of siliceous sponges to other benthic fauna. Siliceous sponges are more likely to be observed as disarticulated spicules altered to nodular or bedded chert, than as a discrete fossil occurrence. A detailed assessment of Permian series cherts from across western North America found that siliceous sponge spicules were a primary sediment component in both nodular and bedded chert strata (Murchey 2004). Because of the lack of sponge body fossils and the relationship between siliceous sponge spicules and nodular and bedded cherts, we use the presence of chert to indicate close proximity to the source of biosiliceous sedimentary producers, which are the sponge animals themselves.

Past work and direct observations (Yochelson and Van Sickle 1968; Murchey 2004; Matheson and Frank 2020; Wistort et al. 2022) lead to our primary hypothesis with regard to biotic reorganization and what role, if any, siliceous sponges played in shaping benthic paleoecologic structure in the Phosphoria Basin. We predict that the presence of siliceous sponges and biosiliceous substrate influenced the recruitment of benthic fauna. We expect that analysis of paleocommunity structure will reveal that fossil collections associated with cherty strata are composed of benthic communities distinct from those of other lithologies.

Stratigraphy and Paleogeography.—The Permian series of the Phosphoria Basin includes the Park City Formation, the Park City Group, the Phosphoria Formation, and the Shedhorn Formation (Cressman 1955; McKelvey et al. 1959; Sheldon 1963; Fig. 1). These units extend laterally over considerable distances and commonly interfinger with one another; hence, the entirety of the Phosphoria Basin and its strata are broadly referred to as the Phosphoria Rock Complex. The Phosphoria Rock Complex was deposited in an epicratonic embayment to the east of the McCloud Volcanic Arc and Havallah Basin (from west-central Nevada to the northwestern United States) and to the west of the subsequent Ancestral Rocky Mountain uplift (Wardlaw 1979; Miller 1987; Blakey 2003; Dickinson 2004). Water depths in the Phosphoria Sea deepened westward from western Wyoming and southern Montana toward southern and central
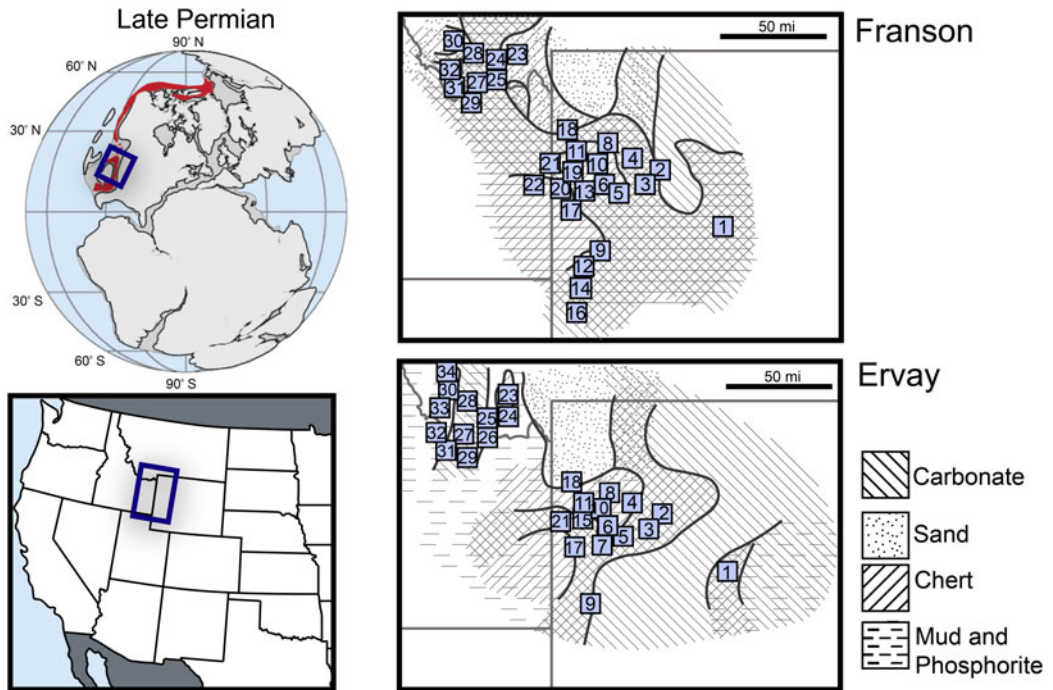
FIGURE 1. Top left, arrangement of the continents during the late Permian; the Phosphoria sea was located in subtropical to tropical paleolatitudes; approximate Phosphoria extent indicated by dark blue box (modified from Ritterbush 2019). Bottom left, map of the western United States; study area indicated by dark blue box. Right, maps of primary lithology of rocks in the Franson and Ervay depositional cycles (modified from McKelvey et al. 1959; Sheldon 1963; Cressman and Swanson 1964); fossil-collecting localities are indicated by light blue numbered squares. Reference numbers correspond to locality names (Supplementary Material 1).

Idaho. The Phosphoria Basin is deposited in three major cycles that equivocally correlate with three Permian third-order eustatic sea-level fluctuations (McKelvey et al. 1959; Whalen 1996; Hendrix and Byers 2000). These cycles, named after the highstand systems tract carbonates of the Park City Formation, are the Grandeur cycle, Franson cycle, and Ervay cycle (Hendrix and Byers 2000).

The Park City Formation includes, from bottom to top, the Grandeur Member, the Franson Member, and the Ervay Member (McKelvey et al. 1959; Fig. 2). These three units generally represent a shallow-marine, carbonate, highstand depositional system tract with varying amounts of carbonate replacement by the precipitation of nodular to bedded cherts (McKelvey et al. 1959; Sheldon 1963; Yochelson and Van Sickle 1968; Hendrix and Byers 2000). The Phosphoria Formation includes, from bottom to top, the Lower Chert, Meade Peak Phosphatic Shale Member, Rex Chert Member,

Retort Phosphatic Shale Member, Cherty Shale, and Tosi Chert Member (McKelvey et al. 1959; Sheldon 1963; Cressman and Swanson 1964; Yochelson and Van Sickle 1968). These units represent a lowstand to transgressive systems tract lithologically characterized by mudstones with ample production of authigenic phosphates and nodular to bedded cherts (Sheldon 1963). The Shedhorn Formation is primarily composed of siliciclastic strata and interfingers with units of both the Phosphoria Formation and the Park City Formation. The shallow-marine sandstones characteristic of the Shedhorn Formation are present in the study area in two major tongues: the Lower Shedhorn and the Upper Shedhorn (Sheldon 1963; Cressman and Swanson 1964; Yochelson and Van Sickle 1968). All units of the Phosphoria Rock Complex intercalate around transition zones, making precise definition of bounding surfaces or even transitions between specific units difficult (Whalen 1996).
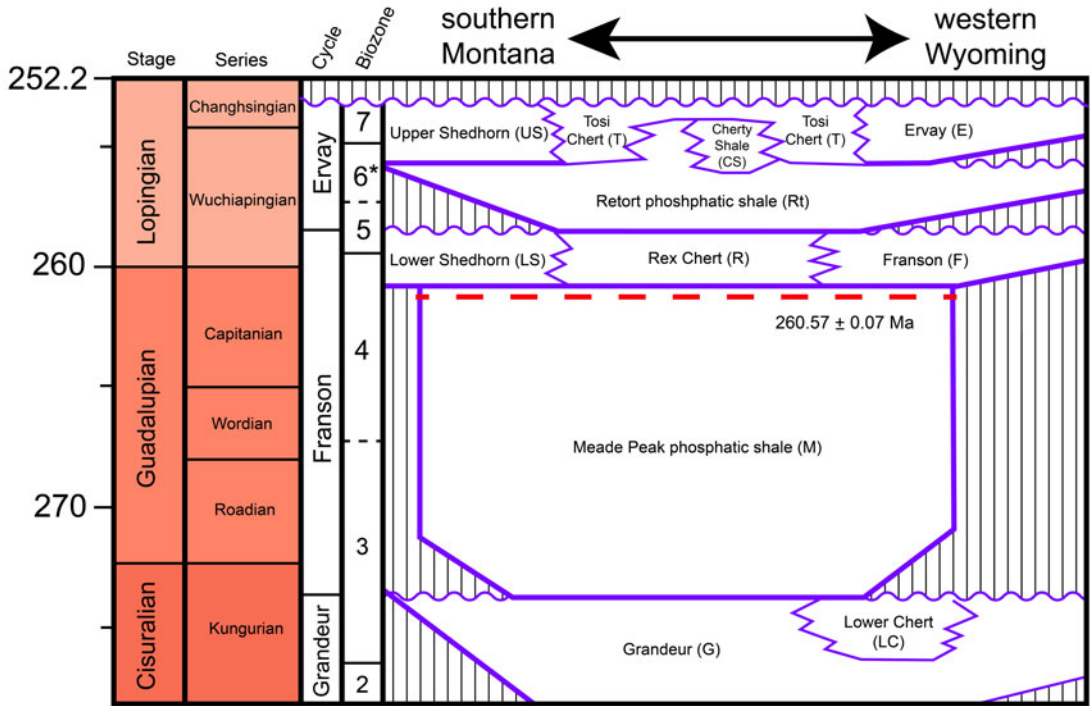
FIGURE 2. Simplified chronostratigraphy of the Phosphoria Basin (modified from Sheldon 1963; Wardlaw 2015; Davydov et al. 2018. The Phosphoria in the study area is deposited in three depositional cycles: Grandeur, Franson, and Ervay. Biozones are adapted from the Wardlaw and Collinson (1986) conodont and brachiopod biozonation scheme; however, this scheme has been rescaled using the 260.57 ± 0.07 Ma zircon age date near the top of the Meade Peak reported by Davydov et al. (2018) (indicated by red dashed line). Discrepancies between the absolute age and the biostratigraphy within the Phosphoria Basin is at present equivocal and requires continued study to resolve.

Methods and Data

We assessed the relationship between paleo-community and lithology using fossil collections digitized from Yochelson and Van Sickle (1968), which comprises more than 1500 individual collections made throughout the Phosphoria Basin. Major benthic faunal groups present in the Phosphoria Basin include brachiopods, bivalves, bryozoans, and gastropods. Minor contributions from anthozoans are also present. Fossils were collected from both outcrops and trenches in Wyoming, Montana, and Idaho (Supplementary Material 1). Yochelson and Van Sickle (1968) report that no consistent method for sampling abundance was implemented between collectors; however, the authors note that relative abundances of fossils remain constant from locality to locality. We filtered the digitized data to include only fossil

collections with detailed lithologic descriptions (Sheldon 1963; Cressman and Swanson 1964). Facies assignments were made using these lithologic descriptions. Filtering the data by these criteria produced a subset of 228 fossil collections and 69 taxa from 35 localities (Fig. 1, Tables 1 and 2, Supplementary Material 1).

Faunal charts from Yochelson and Van Sickle (1968) tabulate fossil collections using a semi-quantitative abundance scheme: A, abundant, more than 16 individuals; C, common, 6 to 15 individuals; R, rare, 1 to 5 individuals; X, present, used to refer to remains that are disarticulated and difficult to count (e.g., disarticulate bryozoan branches or crinoid columnals); and NA, absent. For statistical analyses, these have been converted to the following numerical values: A = 4; C = 3; R = 2; X = 1; NA = 0 (Supplementary Material 1). Because of this

TABLE 1.   Taxon names and associated taxon codes.

Brachiopoda		Bivalvia		Gastropoda	
Code	Taxon	Code	Taxon	Code	Taxon
Ba	*Bathymyonia*	Ac	*Acanthopecten*	Bab	*Babylonites*
Ca	*Cancrinella*	An	*Annuloconcha*	Be	*Bellerophon*
Ch	*Chonetes*	As	*Astartella*	be	Bellerophontacean
Co	*Composita*	AvPec	*Aviculopecten*	Ed	*Edmondia*
De	*Derbyia*	AvPin	*Aviculopinna*	Eu	*Euphemites*
dic	Dictyoclostid	Con	*Concardium*	Euph	*Euphemitopsis*
Di	*Dielasma*	Cos	*Costatoria*	hsg	High-spired gastropods
Ec	*Echinauris*	Cy	*Cyrtorostra*	Kn	*Knightites*
Hu	*Hustedia*	Gi	*Girtypecten*	lsg	Low-spired gastropods
Hy	*Hystriculina*	My	*Myalina*	na	Naticiform
Ju	*Juresania*	Nu	Nuculid	Na	*Naticopsis*
Le	*Leptodus*	NUC	*Nuculopsis*	pl	Pleurotomariacean
Ling	*Lingula*	Pa	Parallelodontid	Tr	*Trachydomia*
lino	Linoproductid	pec	Pectenoid		
Lio	*Liosotella*	per	Permophorid		Echinodermata
Neo	*Neospirifer*	Pe	*Permophorus*	Cr	Crinoid columnals
Orb	*Orbiculoidea*	Po	*Polidevcia*		
phr	Phricodothyrid	Ps	*Pseudomonotis*		Bryozoans
Pro	Productid	Sca	*Scaphellina*	fen	Fenestrate
Sph	*Sphenosteges*	Sch	*Schizodus*	ram	Ramose
spi	Spiriferid	Str	*Streblochondria*		
Spi	"*Spiriferina*"	Stu	*Stuchburia*		Anthozoa
Sq	*Squamaria*	Wi	*Wilkingia*	conu	Conularid
We	*Wellerella*			hor	Horn coral
Ya	*Yakovlevia*				

semiquantitative scheme, when presenting our results, we use the terms "frequent" or "occurrence" in reference to the total collections with a given taxon, and "abundance" in reference to the taxon's semiquantitative code (see "Faunal Composition").

When possible, taxa were identified to the species level (Yochelson and Van Sickle 1968). For statistical analyses, we aggregate any species-level taxa to genus with the

exception of any dubious taxon entries (typically denoted with a question mark) in Yochelson and Van Sickle's (1968) faunal charts. These entries were removed from this study. Semiquantitative abundances were aggregated by taking the highest abundance category of the aggregate fossil entry at a particular generic level. For example, if a particular sample includes a genus with three species with abundance categories of C, R,

TABLE 2.   Summary table of fossil collections (including singletons) that occur in each depositional environment subdivided by formation and chert type.

Cycle	Formation	Abrev.	Facies				Chert type			
			Inner	Mid	Outer	Total	Bedded chert	Nodular chert	Both	Total
Ervay	Ervay	E	6	9	0	15	0	10	0	10
	Upper Shedhorn	US	6	2	0	8	0	4	0	4
	Tosi Chert	T	1	4	1	6	3	1	0	4
	Retort	Rt	4	9	57	70	2	0	0	2
	Cherty Shale	CS	0	1	0	1	0	0	0	0
Franson	Franson	F	19	44	1	64	0	16	0	16
	Lower Shedhorn	LS	9	4	0	13	0	1	0	1
	Rex Chert	R	2	2	2	6	4	0	0	4
	Meade Peak	M	1	12	9	22	0	0	0	0
Grandeur	Grandeur	G	6	13	0	19	3	1	1	5
	Lower Chert	LC	1	2	1	4	3	0	1	4
	Total		55	102	71	228	15	33	2	50

and R, then the aggregate abundance category for that genus would be C.

A fossil collection's lithology was defined based upon the dominant lithology in its lithologic description (Supplementary Material 1). Lithologic descriptions containing chert, either as nodular in a host rock or as bedded chert, were classified as chert. This inclusive definition of chert is appropriate, as we seek to identify how biosiliceous sedimentation, preserved as chert, contributes to classically dominant lithologies (e.g., siliciclastics and carbonates). See "Lithology and Facies Categorization" for a comparison of nodular cherts versus bedded cherts.

A composite cool-water carbonate ramp and glass ramp model was used to categorize fossil collections by detailed lithologic description (James 1997; Gates et al. 2004; Blomeier et al. 2013; Table 2). Fossil collections were categorized into three facies: inner ramp, mid-ramp, and outer ramp. The inner-ramp depositional environment is defined as coarse to fine sand-size clasts composed of bioclasts, quartz, or peloids with thick to indeterminate bedding, and light-colored, nodule to massive chert. The mid-ramp depositional environment is defined as fine sand- to silt-size clasts composed of bioclasts, quartz, or peloids with indeterminate to medium bedding, and light-gray to medium gray, nodular to massive cherts. The outer-ramp depositional environment is defined as silty to argillaceous, with limited bioclasts and quartz, thin to medium or irregular bedding, and medium-gray to dark-gray, nodular to bedded chert. Total fossil collections from each depositional environment were: inner ramp, 55; mid-ramp, 102; and outer ramp, 71 (Table 3). The two most-sampled units in this analysis are the Franson Member (64 collections) and the Retort Phosphatic Shale member (70 collections). These two units account for approximately half of all fossil collections analyzed in this study.

The community matrix was filtered to include only taxa that occur in at least two different collections and collections that have at least two different taxa. This further reduced the data to 105 fossil collections and 49 taxa. This procedure filters all collections of the Lower Chert, Rex Chert, and Cherty Shale from the community matrix. The Lower Chert

TABLE 3. Results of PERMOVA test performed on "all" data, Franson cycle subset, and Ervay cycle subset.

PERMOVA ("all")				
	R^2	F-statistic	df	p-value
Formation	0.22	4.47	7	0.001 ***
Facies	0.03	2.01	2	0.008 **
Lithology	0.03	1.60	3	0.014 *

PERMOVA (Franson cycle)				
	R^2	F-statistic	df	p-value
Biofacies	0.24	7.17	2	0.001 ***
Lithology	0.04	0.78	3	0.816
Formation	0.04	1.19	2	0.212
Facies	0.03	0.96	2	0.523

PERMOVA (Ervay cycle)				
	R^2	F-statistic	df	p-value
Biofacies	0.23	12.73	2	0.001 ***
Facies	0.18	9.87	2	0.001 ***
Lithology	0.12	4.62	3	0.001 ***
Formation	0.08	2.85	3	0.001 ***

and Cherty Shale are undersampled compared with the other units in the Phosphoria Rock Complex. The Grandeur contains many singletons. For some multivariate analyses, we subset the data by depositional cycle to explore how community structure changed through time. In these analyses, we use the same filtering procedure as for the entire dataset. This resulted in 49 collections and 32 taxa in the Franson cycle and 56 fossil collections and 32 taxa in the Ervay cycle

All plots and statistical analyses were performed in R (v. 4.0.4 [15 February 2021], Lost Library Book). The R package vegan was used to calculate distance matrices (Bray-Curtis similarity coefficient) and to perform detrended correspondence analysis (DCA), nonmetric multidimensional scaling (NMDS) ordinations, and permutational analysis of variance (PERMOVA) analyses. Both DCA and NMDS were performed to confirm that a community matrix using semiquantitative abundance resulted in similar plots of fossil collections and centroids in their respective ordination spaces. Hierarchical clustering and heat maps were generated with the package pheatmap using the method *average*, which corresponds to the unweighted pair-group method with arithmetic averaging method.
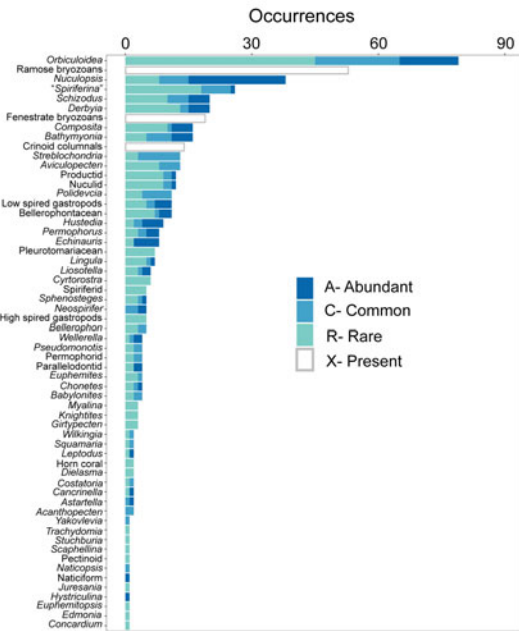
FIGURE 3. Taxa ranked by frequency of fossil collections in which they occur, with the semiquantitative categories (abundant, common, rare, and present) denoted.

Results

Faunal Composition.—The linguloid brachiopod *Orbiculoidea* (79 occurrences) occurs most frequently in these collections (Fig. 3). It is present in every lithologic category and is the most frequent taxon in both siliciclastic and phosphorite lithologies (Fig. 4). Although frequent, *Orbiculoidea* is typically rare. Other frequent brachiopod taxa include the spiriferinid "*Spiriferina*" (26) and orthotetid *Derbyia* (20). *Derbyia* is typically more abundant than "*Spiriferina*." Frequent bivalves include the nuculid *Nuculopsis* (38) and trigoniid *Schizodus* (20). *Nuculopsis* is typically abundant, similar to the productid brachiopod *Echinauris* (8). Ramose (53) and fenestrate (19) bryozoans are frequent. Gastropod taxa occur less frequently than taxa of other major groups. Bellerophontaceans (11) and the indeterminate low-spired gastropods (11) are the most frequent gastropod taxa in the dataset.

To observe changes in faunal occurrences and abundances between different lithologies, we subdivided occupancy by lithology (Fig. 4). Siliciclastic fossil collections frequently contain bivalve and gastropod taxa, with the exception of *Orbiculoidea* (36). *Nuculopsis* (23) is frequent and typically abundant. Occurrences sharply decline after *Orbiculoidea* and *Nuculopsis*. Other frequent bivalve taxa include *Streblochondria* (11) and *Polidevcia* (6); both are of common abundance. Low-spired gastropods (7) are the most frequent gastropod taxon and are typically abundant. Fenestrate bryozoans (4) are infrequent.

In contrast to siliciclastics, carbonates are more evenly distributed. Carbonate fossil collections frequently contain bryozoan and brachiopod taxa. Ramose bryozoans (28) are the most frequent taxon. Frequent brachiopod taxa include *Orbiculoidea* (15), "*Spiriferina*" (13), and *Composita* (11). These three taxa are typically rare. Less frequent brachiopod taxa include *Bathymyonia* (9), *Derbyia* (9), and *Echinauris* (6). Both *Bathymyonia* and *Echinauris* are typically abundant. *Schizodus* (7) and bellerophontaceans (7) are the most frequent bivalve and gastropod taxa, respectively.

Phosphorites are similar to siliciclastics in the dominance of *Orbiculoidea* (15) and *Nuculopsis* (9). However, phosphorites have fewer taxa overall than other lithologies. The majority of phosphorites occur in condensed, outer-ramp mudstones and shales, which rapidly weather in rock outcrop (Yochelson and Van Sickle 1968). For this reason, fossil collections recovered from phosphorites are typically sampled from mining trenches made available to the USGS during the 1950s. Our preparation of the data also excludes fossil collections from south-central Idaho, the depocenter of the Meade Peak Phosphatic Shale. Fossil collections from this area did not have sufficient lithologic descriptions for use in this study. The restricted diversity is in agreement with observations of phosphorites across the Phosphoria Rock Complex (Yochelson and Van Sickle 1968).

Cherts are similar to carbonates, as brachiopod and bryozoan taxa are frequent in both lithologies. Ramose bryozoans (21), *Orbiculoidea* (13), and "*Spiriferina*" (11) are the three most frequent taxa. These two lithologies differ in the occurrence and abundance of accessory brachiopod taxa. In contrast to carbonates, *Derbyia* (8) and *Hustedia* (4) are both more
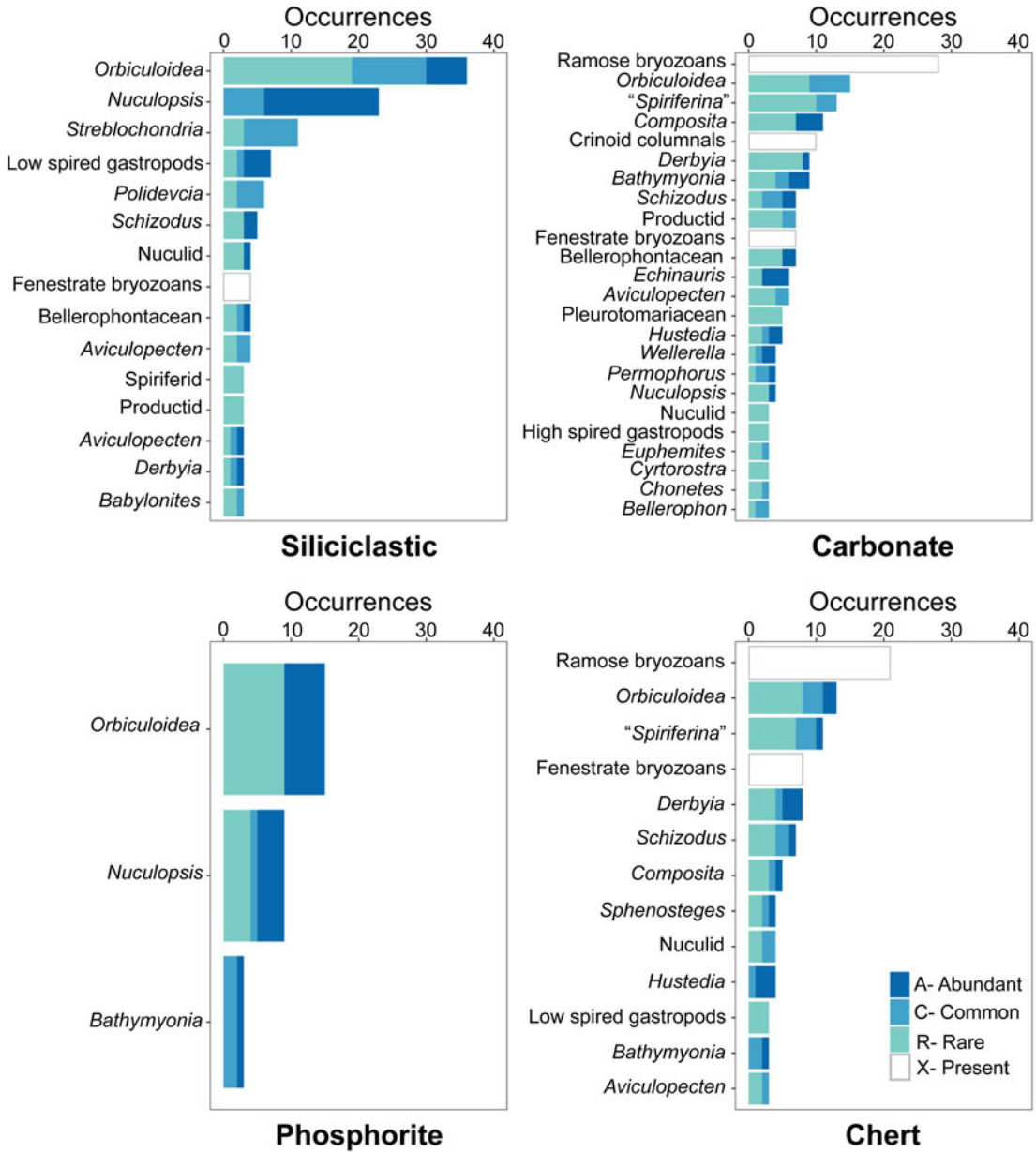
FIGURE 4. Taxa ranked by frequency of fossil collections in which they occur, filtered to include only taxa with a minimum of three occurrences, and subdivided into a collections-associated lithology. The semiquantitative categories (abundant, common, rare, and present) are noted.

abundant and *Composita* (5) and *Bathymyonia* (3) are rarer in cherts. *Schizodus* (7) and low-spired gastropods (3) are the most frequent bivalve and gastropod taxa, respectively; both are typically rare.

Lithology and Facies Categorization.—We sorted fossil collections into three facies based upon their lithologic descriptions (Sheldon 1963; Cressman and Swanson 1964) (Table 2). Facies categories are: inner ramp, mid-ramp, and outer ramp. Mid-ramp is the most frequent facies in these data. Of the three depositional cycles, the Grandeur and Franson cycles contrast with the Ervay cycle. In the Grandeur

and Franson cycles, the majority of fossil collections are sampled from the mid-ramp facies. In the Ervay cycle, the majority of fossil collections are sampled from the outer-ramp facies. The most sampled formations are the Franson Member and the Retort Phosphatic Shale Member. The Franson is primarily composed of inner- to mid-ramp carbonates, while the Retort is primarily composed of outer-ramp siliciclastics and phosphorites.

Two styles of chert preservation are present in rock outcrops of the Phosphoria Rock Complex: bedded cherts and nodular cherts. Bedded cherts are rocks in which the entirety of the stratum is composed of chert, whereas nodular cherts are those in which chert nodules are frequent constituents within a host stratum of a different lithology. In total, 50 fossil collections are classified as chert. Of those, 33 collections are of the nodular type, and 15 collections are of the bedded type; 2 collections have lithologic descriptions in which both types are present. Nodular chert is more frequent in both the Franson (16 occurrences) and Ervay (10), and bedded cherts are more frequent in the Tosi Chert (3), Rex Chert (4), Grandeur (3), and Lower Chert (3). With regard to nodular cherts, the host rock is most frequently carbonate (23) (e.g., carbonate rock, dolomite, or limestone). Other host rocks are sandstone (5) and mudstone (5). Nodular cherts have 25 collections that are not singletons, and bedded cherts have only 2 collections. This indicates the chert signal in these data favors the nodular chert type.

Faunal composition varies between the two chert types. In bedded cherts, *Orbiculoidea* (6 occurrence), *Schizodus* (3), and nuculids (1) are most frequent, and both *Orbiculoidea* and *Schizodus* are abundant. In nodular cherts, Ramose bryozoans (20), "*Spiriferina*" (10), *Derbyia* (8), and fenestrate bryozoans (8) are most frequent, and *Derbyia*, *Hustedia*, and *Echinauris* are abundant.

It is important to further elaborate the connection made between chert and substrate. Chert is diagenetic, but it originates primarily from the burial of biosiliceous skeletal elements (e.g., tests, frustules, and spicules) (Knauth 1979, 1994; Schubert et al. 1997; Kidder and Erwin 2001; Kidder and Tomescu 2016; Maldonado et al. 2019). In these analyses, we make the

assumption that more biogenic silica in the substrate, predominantly sponge spicules in this region of the Phosphoria Rock Complex (Murchey 2004), is equivalent to chert, whether it is nodular, bedded, or both. Chert is thought to alter and precipitate early on in diagenesis, exemplified by its association with both body and trace fossils (Bromley and Ekdale 1984; Maliva and Siever 1989; Wistort et al. 2019). We draw the connection that biosiliceous deposition likely has an impact on substrate due to the abundance of spicular cherts in the Phosphoria Rock Complex, and the presence of chert is the best available data to track this.

Ordination Results.—Multivariate ordinations were utilized to explore the relationships among formation, facies, and lithology with respect to faunal composition of fossil collections. Previous paleoecologic studies have demonstrated that biotic gradients in community data can elucidate the environmental parameters that influence them. (Holland et al. 2001; Holland 2005; Holland and Patzkowsky 2007; Clapham and James 2008; Patzkowsky and Holland 2012). The environment influences both recruitment and survivorship of marine taxa and can control community structure via a variety of parameters (hydrodynamic energy, oxygenation, photic energy, and substrate consistency, etc.) (Holland and Patzkowsky 2007; Patzkowsky and Holland 2012). Previous studies have suggested water depth as a primary control on community composition; however, water depth covaries with environmental parameters and thus is not necessarily the cause of biotic gradients. For a thorough review of biotic and environmental gradients in marine paleoecology, please see Patzkowsky and Holland (2012).

DCA and NMDS analyses were performed and fossil collections were coded for their membership in three categories: formation, facies, and lithology (Fig. 5). Formation centroids do not shift considerably between plots of the two ordination methods, with the exception of the Meade Peak Phosphatic Shale Member and Tosi Chert Member. In both plots, the Franson Member, Ervay Member, and Lower Shedhorn plot closely in ordination space at low scores of axis 1. These three formations are composed of shallow-water carbonates and

siliciclastics. The Retort Phosphatic Shale Member and the Upper Shedhorn member plot closely in ordination space at high scores of axis 1 in both plots. The Retort is commonly composed of offshore siliciclastics and phosphorites, but the Upper Shedhorn is composed of nearshore siliciclastics. In the DCA ordination space, the Upper Shedhorn plots at more intermediate values proximal to the Grandeur Member. In the NMDS ordination space, the Upper Shedhorn plots at high scores of axis 1 proximal to the Retort. This indicates fauna of the Upper Shedhorn must be transitional between the mid-ramp, carbonate-dominant Grandeur fauna and the outer-ramp, siliciclastic- dominant Retort fauna. The Tosi Chert Member centroid varies in relative position in ordination space between these two plots. In the DCA ordination space, the Tosi Chert plots well within the carbonate-dominant shallow-water fossil collections at low axis 1 scores. In the NMDS ordination space, the Tosi Chert plots at intermediate axis 1 scores, the transitional zone between the inner/mid- and outer-ramp collections, similar to the Upper Shedhorn.

Facies centroids separate strongly into two end-members along axis 1 of both plots. Fossil collections from outer-ramp facies have high scores along axis 1 in contrast with collections from inner- and mid-ramp facies that have low scores along axis 1. Centroids of the inner-ramp and mid-ramp facies plot close together in ordination space, indicating very similar faunal compositions. This is unexpected, as commonly in paleoecologic studies there is more significant separation along a nearshore to offshore gradient corresponding with the primary axis of variance. Little segregation between the taxa of the inner-ramp and mid-ramp facies may reflect homogeneous environmental conditions. Also, the position of the Upper Shedhorn Member is suspect. This unit is entirely composed of inner-ramp facies, but it plots proximal to the outer-ramp centroid. Axis 2 appears to have little impact on the segregation of facies groupings in ordination space.

Similar to facies, lithology centroids separate strongly into two end-members along axis 1 of both plots. Siliciclastic and phosphorite lithologies are more frequent at high axis 1 values,

while carbonate and chert lithologies are more frequent at low axis 1 values. This separation between lithologies is weaker than the separation between outer-ramp and inner/mid-ramp facies. Although more densely concentrated at these end-members, all lithologies are present across axis 1 in both plots. Along axis 2, phosphorites tend to occur at higher scores, with the exception of a lone outlier at low values of axis 2. This outlier skews the phosphorite centroid toward intermediate axis 2 values, particularly in the NMDS plot.

To interpret the distribution of fossil collections in ordination space, we plotted taxon scores. Taxa that are farther from the center are most abundant in the collections in that area of the ordination space. In both ordination spaces, the bivalves *Nuculopsis* and *Streblochondria*, as well as the gastropod *Babylonites*, plot at high scores of axis 1, corresponding with the outer-ramp facies and the phosphorite and siliciclastic lithologies. A mix of gastropod and bivalve taxa plot at intermediate values of axis 1 in both plots. Brachiopods, bryozoans, and crinoids plot at low to intermediate values of axis 1 corresponding with the inner/mid-ramp facies and the carbonate and chert lithologies. Important taxa in this part of the ordination space include the brachiopods *Sphenosteges*, *Dielasma*, *Liosotella*, and *Echinauris*; the bivalve *Myalina*; and ramose bryozoans. Interestingly, in the DCA plot, ramose bryozoans and the brachiopod "*Spiriferina*" plot at more intermediate axis 1 scores in contrast with the NMDS plot, in which these taxa plot at negative axis 1 scores. These two taxa more strongly contribute to the arrangement of fossil collections in the NMDS analysis.

Along axis 2 in both ordination spaces, gastropods *Knightites* and *Euphemites* and large, shallow-water bivalves *Aviculopecten* and *Schizodus* plot at low scores proximal to siliciclastic, carbonate, and chert lithologies. Plotting at high axis 2 scores, particularly in the NMDS space, proximal to phosphorite and outer-ramp centroids are the brachiopods *Orbiculoidea* and *Lingula*, the bivalves *Nuculopsis* and *Streblochondria*, and the gastropod *Babylonites* and low-spired gastropods.

A PERMOVA test was performed to assess the influence of coded categories on patterns
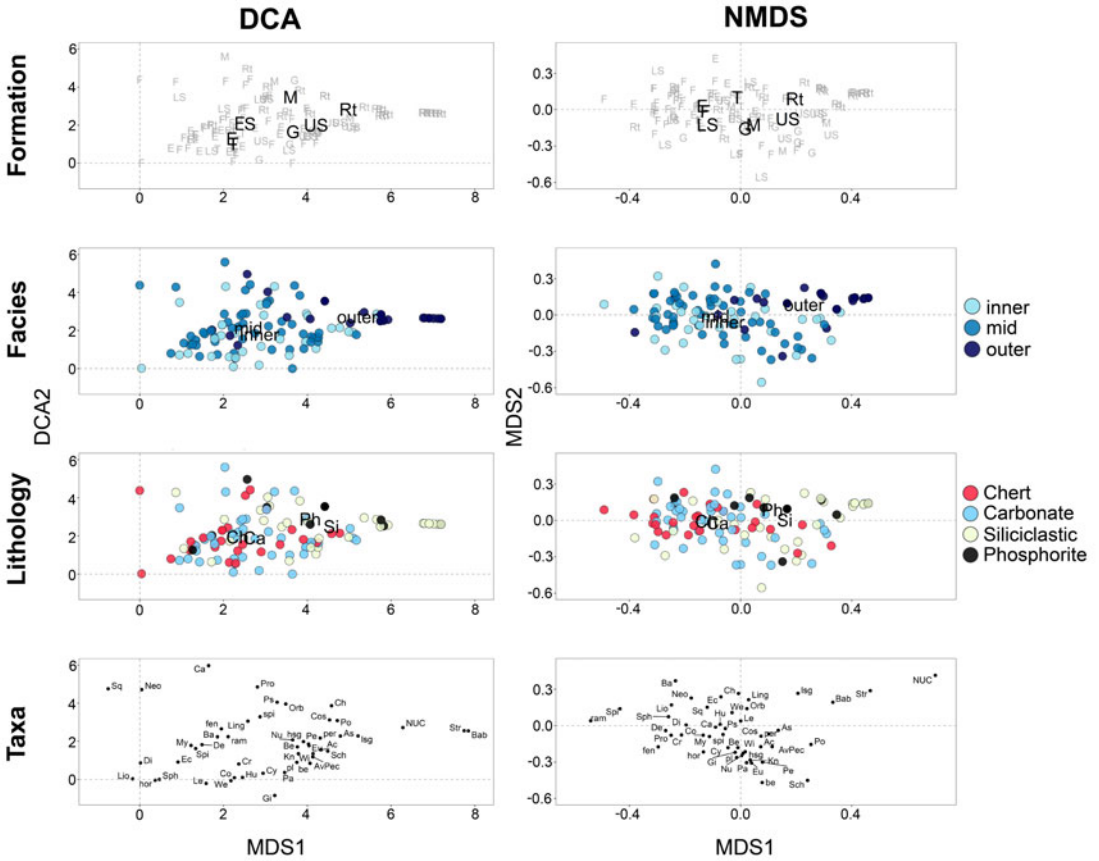
FIGURE 5. Detrended correspondence analysis (DCA) and nonmetric multidimensional scaling (NMDS) ($k = 3$) of all fossil collections in the filtered dataset ("all"; 105 collections). Collections are coded to the categories of facies, lithology, and taxa. The letter corresponds to the formation code (see Table 2). The shape of collections corresponds to facies. The color of collections corresponds to lithology. The black bold text in each plot corresponds to that plot's category centroids. Formations are labeled by formation code; facies by facies name: inner ramp, mid-ramp, or outer ramp; and lithology by lithologic code: Ch, chert; Ca, carbonate; Si, siliciclastic; and Ph, phosphorite. Taxon scores are plotted as points with their associated taxon code (see Table 1).

in the arrangement of fossil collections across ordination space (Table 3). The coded categories of formation, facies, and lithology were compared using the "all" community matrix (this corresponds with the data presented in Fig. 5). The formation category contributed to 22% of variance of the community matrix, while facies and lithology contributed to 3% each. This statistical test is supported by the proximity of formation centroids from different depositional cycles, such as Franson, Ervay, and Lower Shedhorn or Retort and Upper Shedhorn. A single category contributing to more than 20% of variance is quite large

when dealing with ecologic data. This result indicates that membership in a particular formation, and probably in a particular systems tract, significantly affects the arrangement of fossil collections in ordination space to the point that formations of similar character plot more closely together, overcoming any signal of lithology or facies. Because of this, it is difficult to disentangle the potential effects of these latter categories on community data.

To mitigate the effect of formation membership on the ordination space, we separated the community matrix into the Franson cycle and Ervay cycle and performed NMDS

analyses on both subsets (Fig. 6). Ordination analysis was not performed on the Grandeur cycle (e.g., Grandeur Member and Lower Chert), as there are too few fossil collections to draw any meaningful conclusions. Fossil collections were again coded for their membership in three categories: formation, facies, and lithology.

Formation centroids in the Franson cycle ordination space separate along MDS1. The Franson Member centroid plots at low MDS1 scores, the Lower Shedhorn plots at intermediate scores, and the Meade Peak plots at high scores. The Meade Peak is represented by only two fossil collections in the ordination space, one of which occurs at intermediate MDS1 scores. Fossil collections from the Franson Member plot most frequently in low and intermediate scores of MDS1; however, some samples do plot in high scores. Fossil collections from the Lower Shedhorn plot most frequently in intermediate scores of MDS1, with the exception of a lone outlier that plots in negative values of MDS1.

Formation centroids in the Ervay cycle ordination space also separate along MDS1. The Ervay Member and Tosi centroids plot at high scores on MDS1, and the Retort and Upper Shedhorn centroids plot at low to intermediate scores. The Retort centroid would likely plot at lower MDS1 scores if not for an outlier collection at very high scores. Removal of this collection would probably increase the distance between the Retort and Upper Shedhorn centroids. The Ervay Member, Tosi, and Upper Shedhorn all loosely cluster around their respective centroids. In contrast, fossil collections of the Retort are spread across ordination space with a strong clustering at low MDS1 scores. Along the MDS2 axis, almost all collections from the Tosi and Ervay Member plot at low scores. The Retort and Upper Shedhorn plot at intermediate to high MDS2 scores.

Similar to facies centroids of the "all" dataset (Fig. 5), facies centroids in the Franson cycle ordination space separate into two end-members along MDS1. Fossil collections from the outer-ramp facies have high MDS1 scores in contrast with collections from the inner- and mid-ramp facies, which have low MDS1 scores. Centroids of the inner-ramp and mid-

ramp facies plot close together in ordination space. The lack of fossil collections from the Meade Peak in this analysis makes it difficult to say with confidence that the outer-ramp facies are really distinct form the inner/mid-ramp. Similar to the "all" data, there is little segregation between the taxa of the inner-ramp and mid-ramp facies, which may reflect homogeneous environmental conditions. The MDS2 axis seems to have little impact on the segregation of facies groupings in ordination space.

Facies centroids of the Ervay cycle show a different arrangement, contrasting with those of the "all" data and the Franson cycle. The outer-ramp centroid plots at low MDS1 scores, the inner-ramp centroid plots at intermediate scores, and the mid-ramp centroid plots at intermediate to high scores. This is the only ordination space in which the inner- and mid-ramp fossil collections have distinct centroids, and of particular note is the inner-ramp centroid plotting between the mid-ramp and outer ramp along MDS1. Inner-ramp fossil collections are evenly split between the Ervay Member (6) and the Upper Shedhorn (6). The Upper Shedhorn inner-ramp collections plot at intermediate MDS1 scores proximal to the outer-ramp centroid, whereas the Ervay Member inner-ramp collections plot at high MDS1 scores. This is odd and further illustrates the similarity in faunal composition of the Upper Shedhorn and the Retort. Without this strong similarity in faunas, the inner-ramp centroid would most likely plot closer to the mid-ramp centroid.

Lithology centroids in the Franson cycle separate similarly to those of the "all" data ordinations, in which the carbonate centroid plots proximal to the chert and the siliciclastic centroid plots proximal to the phosphorite. A single sample is categorized as a phosphorite lithology and is a member of the Meade Peak. Lithology centroids in the Ervay cycle separate similarly to those of the "all" data and the Franson cycle ordinations; however, the separation of fossil collections belonging to the carbonate/chert and siliciclastic/phosphorite end-members is much stronger. There is very little overlap in intermediate MDS1 scores of these lithologies compared with the other ordinations. Chert lithologies seem to form a tighter
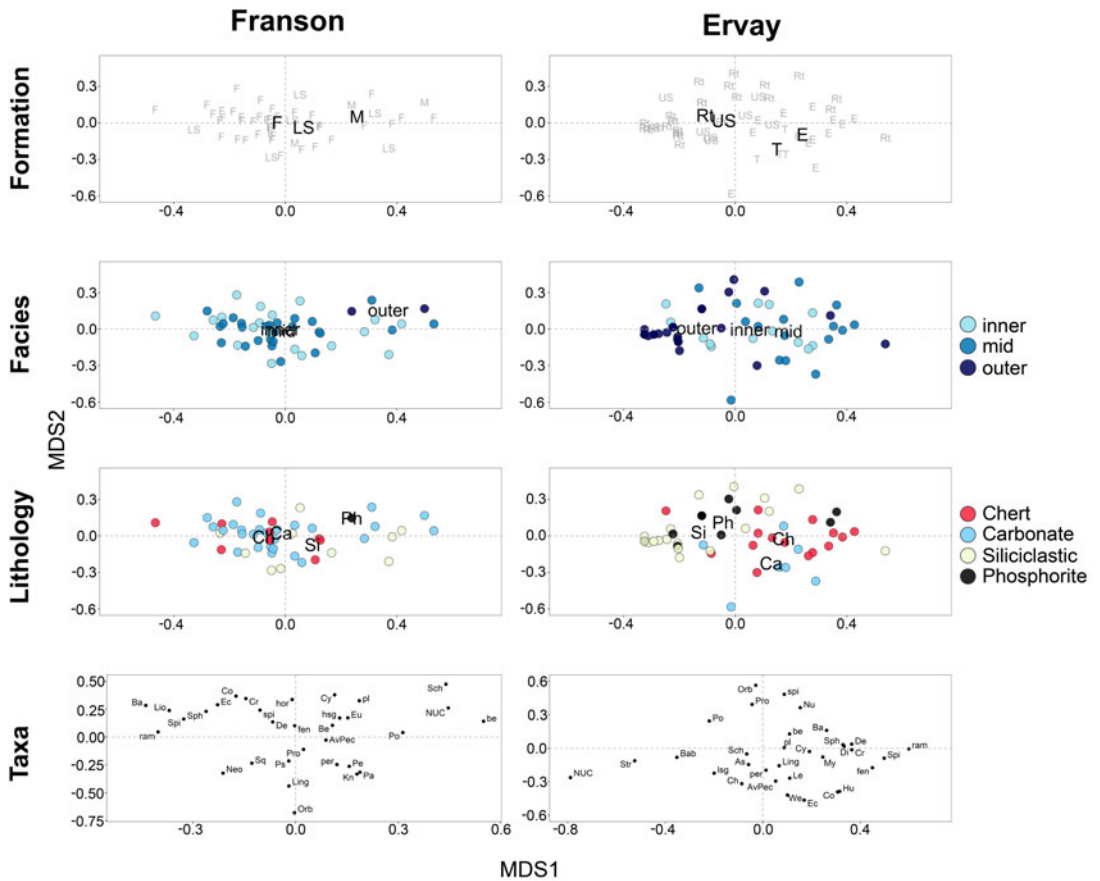
FIGURE 6. Nonmetric multidimensional scaling (NMDS) ordination of Franson cycle (49 collections) and Ervay cycle (56 collections) data. Collections are coded to the categories of facies, lithology, and taxa. The letter corresponds to the formation code (see Table 2). The shape of collections corresponds to facies. The color of collections corresponds to lithology. The black bold text in each plot corresponds to that plot's category centroids. Formations are labeled by formation code; facies by facies name: inner ramp, mid-ramp, or outer ramp; and lithology by lithologic code: Ch, chert; Ca, carbonate; Si, siliciclastic; and Ph, phosphorite. Taxon scores are plotted as points with their associated taxon code (see Table 1).

grouping in the Ervay cycle than in any of the other ordination spaces. Similar to the pattern observed in the "all" data, phosphorite lithologies plot at intermediate to high MDS2 scores, while chert and carbonate collections plot at intermediate to low MDS2 scores.

Taxon scores were plotted for both the Franson cycle and Ervay cycle ordination spaces. In the Franson cycle, the brachiopods *Bathymyonia*, *Liosotella*, "*Spiriferina*," *Sphenosteges*, and *Echinauris*, along with ramose bryozoans, plot at low MDS1 and high MDS2 scores. The bivalves *Nuculopsis*, *Schizodus*, and *Polidevcia*, along with the bellerophontacean gastropods, plot at high MDS1 and high MDS2 scores. The brachiopods

Orbiculoidea, *Lingula*, *Neospirifer*, and *Squamaria*, the bivalves *Permophorus*, parallelodontid, and *Pseudomonotis*, and the gastropod *Knightites* form a loose cluster at intermediate MDS1 scores and intermediate to low MDS2 scores. In the Ervay cycle, the relative position of taxon scores is similar to the Franson cycle. The brachiopods "*Spiriferina*," *Sphenosteges*, *Dielasma*, and *Derbyia*, along with ramose bryozoans and fenestrate bryozoans, plot at high MDS1 scores. Similar to the "all" data ordinations, bivalves *Nuculopsis*, *Streblochondria*, and *Babylonites* plot near one another at low MDS1. *Orbiculoidea*, productids, and spiriferids plot close together at high MDS2 scores.

Hierarchical Clustering Analysis.—To further explore the relationships of taxa and fossil collections in the Franson cycle and Ervay cycle, we generated heat maps to observe how fossil collections clustered with respect to taxon abundance. In both cycles, distinct clusters of fossil collections (biofacies) were formed. Biofacies are defined by significant changes in both taxa and/or abundance.

The Franson cycle clustered into three biofacies that are labeled Franson 1, Franson 2, and Franson 3 (Fig. 7). The Franson 1 biofacies is defined by the brachiopods *Derbyia* and "*Spiriferina*" and ramose bryozoans. These taxa are frequent in samples of Franson 1 but are typically rare. The brachiopods *Bathymyonia* and *Echinauris* are less frequent than the defining taxa but, when present, are typically common to abundant. These taxa both have a weakly concave dorsal valve and a strongly convex ventral valve with dense spines. This biofacies occurs primarily in inner-ramp to mid-ramp carbonates with minor cherts and siliciclastics. This convergence of functional characters may indicate a desirable body plan for living in the inner- to mid-ramp depositional environment, characterized by ample carbonate and biosiliceous sedimentation (frequent carbonate and chert lithologies).

The Franson 2 biofacies is defined by the brachiopods *Orbiculoidea*, *Lingula*, and *Neospirifer*. *Orbiculoidea* and *Lingula* are typically common to abundant and occur in only carbonate and siliciclastic lithologies. *Neospirifer* is less frequent and typically common. It occurs in chert and carbonate lithologies. The brachiopods *Liosotella* and *Composita* are infrequent but, when present, are abundant. Ramose bryozoans occur in Franson 2 less frequently than in Franson 1. Fossil collections in this biofacies are a mix of both inner- and mid-ramp facies and carbonate, chert, and siliciclastic lithologies. Franson 2 shares some similar taxa with Franson 3. These include the bivalves *Permophorus*, *Polidevcia*, and parallelodontids and the gastropod *Bellerophon*. With no distinct facies or lithology and sharing similarities with both the Franson 1 and Franson 3 biofacies, Franson 2 is transitional between these two end-member biofacies of the Franson cycle.

The Franson 3 biofacies is defined by the bivalve *Schizodus* and the gastropod

bellerophontaceans. Both of these taxa are frequent and typically common to abundant. Fossil collections in this biofacies are from every facies and every lithology, with the exception of chert. Carbonate is the dominant lithology. This biofacies also contains both samples of the Meade Peak. No brachiopod or bryozoan taxa occur in this biofacies. These two major groups are frequent and abundant elsewhere in the Franson cycle. This indicates that fossil collections that contain brachiopods and bryozoans are significant to the underlying structure of the Phosphoria Rock Complex community.

The Ervay cycle clustered into three biofacies that are labeled Ervay 1, Ervay 2, and Ervay 3 (Fig. 8). The Ervay 1 biofacies is defined by bivalve *Nuculopsis*, which is both frequent and abundant. The bivalve *Streblochondria* is frequent and common. The bivalves *Polidevcia*, *Aviculopecten*, *Schizodus*, and *Astartella*, the gastropod *Babylonites*, and low-spired gastropods are infrequent and rare to abundant. Similar to the Franson 1 biofacies, brachiopod taxa are very limited. In Ervay 1, *Bathymyonia* and "*Chonetes*" are present in a single fossil collection each, but they are abundant in each of those collections. This biofacies corresponds strongly with the Retort Phosphatic Shale unit, the outer-ramp facies, and the siliciclastic lithology. It illuminates a potential cause of the proximity of the Upper Shedhorn and Retort centroids in Figure 6. Five Upper Shedhorn fossil collections cluster tightly together in the Ervay 1 biofacies. These collections contain the shallow-water bivalves *Aviculopecten* and *Schizodus*, which are also present in the Ervay 3 biofacies. However, these collections also contain abundant *Nuculopsis*. The strength of the abundant *Nuculopsis* when calculating the distance matrix for ordination is what likely pulls the Upper Shedhorn collections toward the Retort centroid in ordination space. If not for the abundant category of *Nuculopsis*, these collections would probably plot in Ervay biofacies 3. This exemplifies one of the limitations of using semiquantitative abundance data.

The Ervay 2 biofacies is defined by the brachiopod *Orbiculoidea*. This brachiopod occurs in all fossil collections of the biofacies and is rare to abundant. This biofacies corresponds strongly with the Retort Phosphatic Shale
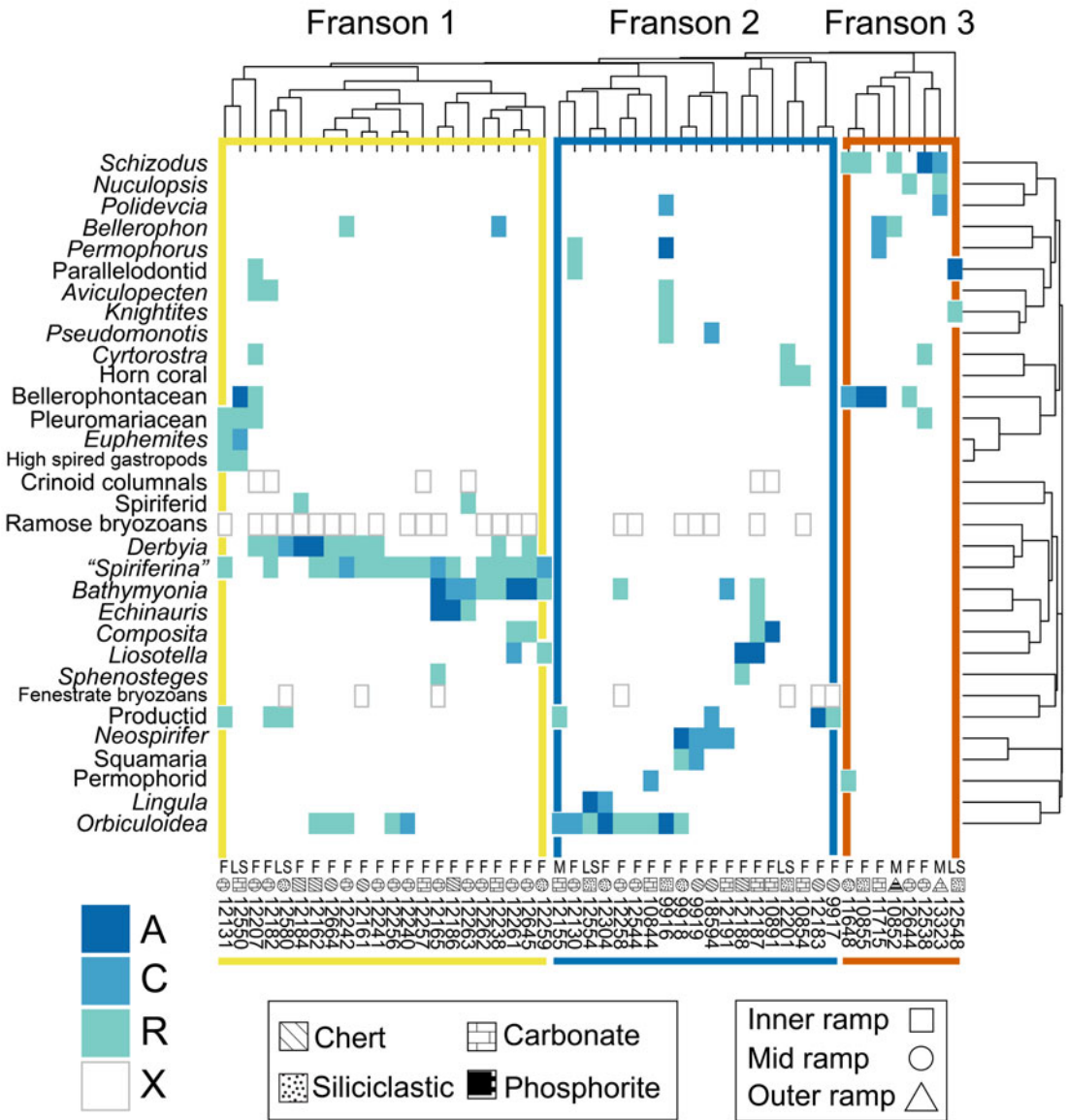
FIGURE 7. Heat map of Q-mode and R-mode hierarchical clustering of taxa vs. fossil collections in the Franson cycle. Shapes of points correspond to depositional environment and pattern fill of points corresponds to lithology. A, C, R, and X correspond to the semiquantitative categories abundant, common, rare, and present, respectively. Results are separated into three biofacies based upon changes in faunal composition and abundance. These biofacies are separated by the three colored outlines and are labeled Franson 1, Franson 2, and Franson 3. The letter corresponds to the formation code (see Table 2).

unit, the outer-ramp facies, and the siliciclastic and phosphorite lithologies. The Ervay 2 biofacies is similar to the Franson 2 biofacies in that *Orbiculoidea* is a defining taxon. However, the Ervay 2 biofacies has a much lower diversity of taxa. It also has a strong affiliation with the phosphorite lithology in contrast to the Franson

2 biofacies, which has more carbonate and chert collections.

The Ervay 3 biofacies is defined by the brachiopods *Composita*, *Hustedia*, and *Echinauris* and ramose bryozoans. These taxa are frequent and abundant. *Derbyia* and *Bathymyonia* are less frequent and rare to abundant. Fenestrate
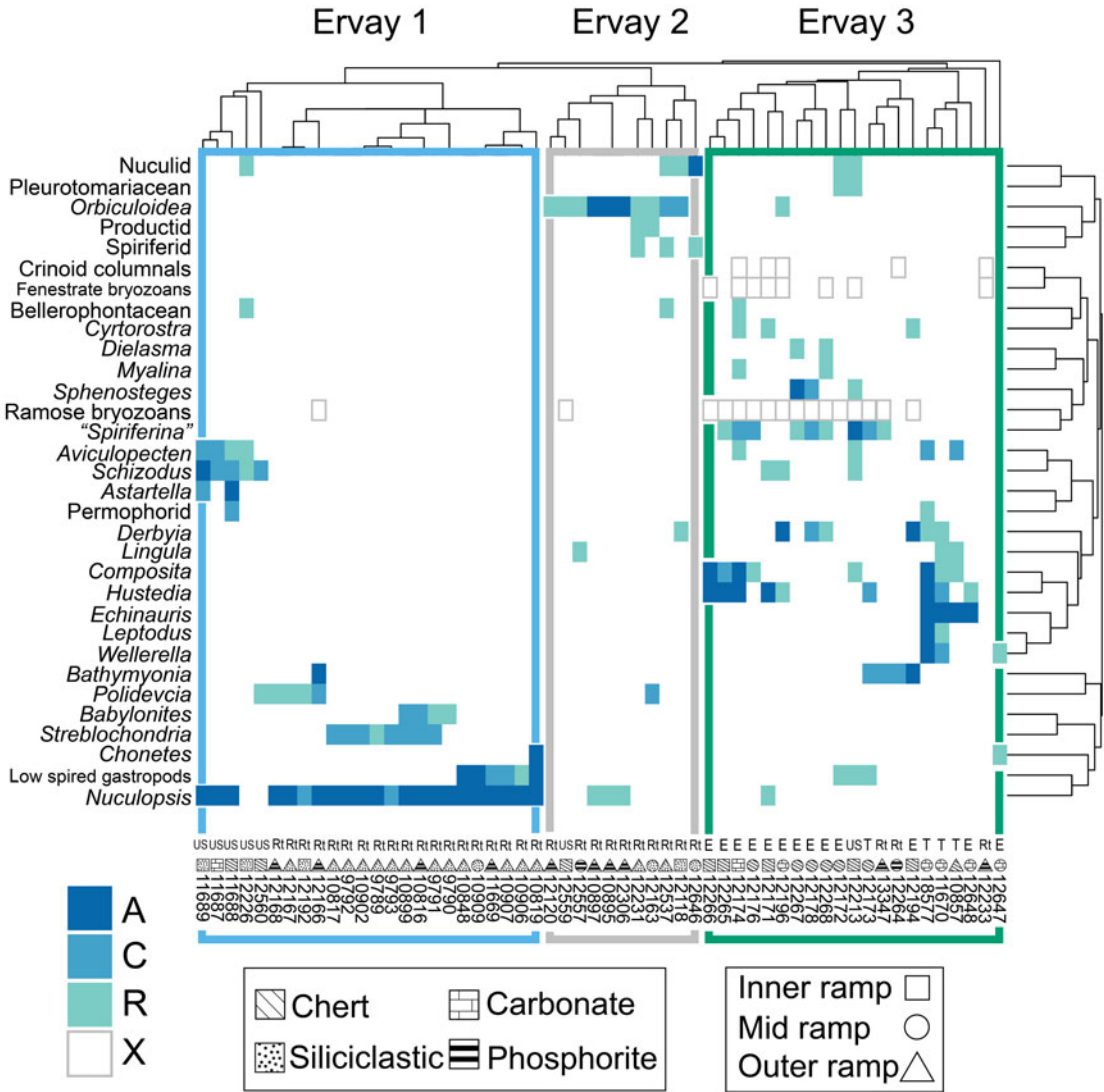
FIGURE 8.   Heat map of Q-mode and R-mode hierarchical clustering of taxa vs. fossil collections in the Ervay cycle. Shapes of points correspond to depositional environment and fill of points corresponds to lithology. A, C, R, and X correspond to the semiquantitative categories abundant, common, rare, and present, respectively. Results are separated into three biofacies based upon changes in faunal composition and abundance. These biofacies are separated by the three colored outlines and are labeled Ervay 1, Ervay 2, and Ervay 3. The letter corresponds to the formation code (see Table 2).

bryozoans and crinoid columnals are also present. This biofacies corresponds with the Ervay Member and Tosi units, the inner- and mid-ramp facies, and the chert and carbonate lithologies. The Ervay 3 biofacies is similar to the Franson 1 biofacies in that it is defined by a diverse fauna of brachiopods and frequent ramose bryozoans. These two biofacies contrast in specific brachiopod taxa and abundances. The most frequent brachiopods in the Franson

1 biofacies are "*Spiriferina*" and *Derbyia*. These two taxa are frequent only in Ervay 3, but typically less abundant than the brachiopod taxa that define the biofacies. *Echinauris* and *Bathymyonia* are abundant in both biofacies. The defining fauna of Ervay 3, *Composita* and *Hustedia*, are infrequent and rare or not present in Franson 1. These biofacies also contrast in dominant fossil collection lithology. In Franson 1, carbonates are the dominant lithology with

minor cherts, whereas in Ervay 3, cherts are the dominant lithology with minor carbonates. The differences between the constituent taxa of these two biofacies exemplify the differences between carbonate and biosiliceous depositional regimes.

To understand how these biofacies fit along a gradient, we coded fossil collections in the ordination spaces of the Franson cycle and Ervay cycle with their respective biofacies memberships and plotted their taxon scores (Fig. 9). Taxon scores are slightly jittered for the sake of readability; this movement is small and does not affect the interpretation of the relative position of scores. The Franson cycle ordination space separates into two end-members that correspond with facies in Figure 6. Plotting at low MDS1 scores are the Franson 1 and Franson 2 biofacies, and at high MDS1 scores is the Franson 3 biofacies. These correspond with the facies centroids in which inner and mid-ramp plot more closely together at low scores and the outer ramp plots at higher scores. These two end-members segregate remarkably cleanly in the ordination space, with the lone exception of a single Franson 1 collection that plots within Franson 3. The Franson 1 and Franson 2 biofacies share many similar taxa; however, Franson 1 forms a tighter cluster within the broader Franson 2. This result indicates a compositional difference between the two communities that may correspond with inner-ramp and mid-ramp communities. We interpret that the Franson 1 biofacies likely correlates with the mid-ramp and Franson 2 with the inner ramp. The presence of a diverse brachiopod fauna along with ramose bryozoans and a generally carbonate lithology fit the expectation of a mid-ramp depositional setting (Blomeier et al. 2013). The brachiopods Lingula and Orbiculoidea occur along with a more diverse gastropod fauna and the only horn corals in the dataset, indicating a likely nearshore depositional setting.

The Ervay cycle's three biofacies separate cleanly in ordination space with no overlap of fossil collections. Along MDS1, Ervay 1 plots at low to intermediate scores, Ervay 2 plots at intermediate scores, and Ervay 3 plots at intermediate to high scores. Along MDS2, Ervay 3 plots at low to intermediate
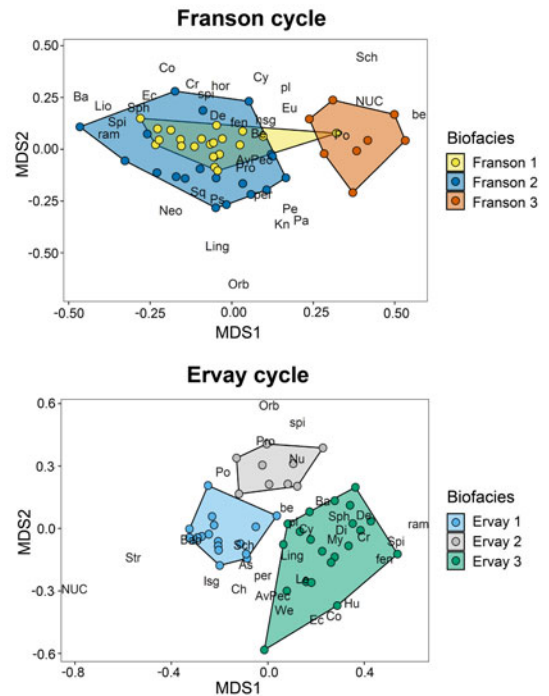

FIGURE 9. Nonmetric multidimensional scaling (NMDS) ordination of the Franson cycle and Ervay cycle (from Fig. 6) coded to biofacies (from Figs. 7, 8). Taxon scores plotted and slightly jittered for readability; this does not significantly change their relative positioning. Convex hulls colored by their associated biofacies.

scores, Ervay 1 plots at intermediate scores, and Ervay 3 plots at high scores. The Ervay cycle ordination space is unique, in that the inner-ramp centroid plots at intermediate MDS1 and MDS2 scores, between the outer-ramp and mid-ramp centroids. Taxa plotting at intermediate scores along MDS1 include the brachiopods Orbiculoidea, Lingula, and productids, the bivalves Cyrtorostra, Aviculopecten, and nuculids, and the gastropods bellerophontaceans and pleurotomariaceans. These taxa all separate along the MDS2 axis in which Orbiculoidea plots at high scores, Lingula plots at intermediate scores, and Aviculopecten plots at low scores. This separation along the MDS2 axis corresponds to broad changes in lithology in the Ervay cycle ordination space. Plotting at high MDS2 scores are a mix of siliciclastic and phosphorite collections from the Retort, and at low MDS2 scores are a mix of chert and carbonate collections

from the Ervay Member and Tosi. Similar to the Franson 2 biofacies, the presence of *Lingula* and *Aviculopecten* could indicate a more nearshore depositional environment; however, in the case of Ervay 3, *Orbiculoidea* plots more closely with Retort outer-ramp than inner-ramp collections. This confounding result may be related to the stark contrast in lithologies. *Orbiculoidea* plots closely to phosphorite collections. Lithology also seems to influence Ervay 3 biofacies along MDS2. The Ervay 3 cluster is closely associated with chert collections with minimal contributions from other lithologies.

A PERMOVA test was performed to evaluate the influence of the coded categories of formation, facies, lithology, and biofacies on patterns in the arrangement of fossil collections in both the Franson cycle and the Ervay cycle ordinations (Table 3). In the Franson cycle, the biofacies category contributed to 24% of the variance in the community matrix. Lithology and formation contributed 4%, and facies 3%. In the Ervay cycle, the biofacies category contributed 23% of the variance in the community matrix, facies 18%, lithology 12%, and formation 8%. In both cycles, the percent of variance attributable to biofacies is high, as biofacies is defined by faunal composition. In the Franson cycle, little variance is explained by lithology, formation, or facies, in contrast with the Ervay cycle, in which each of these factors contributes significantly. This may be due to the overwhelming sampling intensity of the Franson compared with the Lower Shedhorn and the Meade Peak. More fossil collections from these two formations would likely contribute facies in the inner ramp and the outer ramp, which would produce a more well-defined gradient between facies along MDS1. The Ervay cycle is more balanced with regard to sampling intensity. In the Ervay cycle, a significant amount of variance is explained by each of the coded categories. Facies contributes the most to the organization of collections along MDS1. Lithology contributes to the separation of collections along MDS2.

Discussion

In this study, we hypothesized that the presence of siliceous sponges would influence the recruitment of benthic fauna driving faunal composition of benthic communities in the Phosphoria Rock Complex. These data do not strongly support this prediction. Our results demonstrate that chert lithology collections are distinct from siliciclastic collections, which tend to exhibit more gastropod and bivalve taxa. However, faunal composition of chert collections is largely similar to that of carbonate collections. Both lithologies are composed of primarily brachiopod and bryozoan fauna. Brachiopods that are frequent and abundant in both lithologies include *Echinauris*, *Bathymyonia*, *Derbyia*, and "*Spiriferina*." This close association of faunal composition in both chert and carbonate indicates that the increased presence of sponges did not prohibit the recruitment of carbonate mineralizing fauna and had a limited effect on community structure (Ritterbush 2019). As opposed to lithology, facies exerts a greater influence on faunal composition within the Phosphoria Rock Complex.

Cherts Associated with Inner- and Mid-ramp Facies.—In the modern era, deposition of siliceous skeletal material is typically restricted to deep-water upwelling zones and polar currents; however, throughout the Phanerozoic, cherts are recognized in both nearshore and offshore facies (Hesse 1989; Beauchamp and Baud 2002; Murchey 2004; Behl 2011; Rowden 2015). Schubert et al. (1997) proposed that the focus of siliceous deposition in deep-water settings was not always the case during the Phanerozoic but likely shifted from nearshore to offshore with the evolution of diatoms during the Cretaceous. During the late Paleozoic, however, researchers suggest that the locus of biosiliceous deposition occurs in shallow epicratonic seas (Schubert et al. 1997; Kidder and Erwin 2001; Butts and Briggs 2011; Kidder and Tomescu 2016).

Chert and carbonate collections tend to occur closer to the inner- and mid-ramp centroids in all ordinations, implying an association between these lithologies and facies. Previous work in the Phosphoria Basin (Murchey 2004) agrees with our results indicating a nearshore interpretation of biosiliceous deposition. Fieldwork in the Phosphoria Rock Complex confirms these results, in which light gray to blue and purple, nodular and bedded cherts occur frequently in the inner-ramp facies (Matheson and Frank 2020; Wistort et al. 2022).

Carbonate-Chert Faunal Community.—Hierarchical clustering and ordination reveal that chert collections most frequently occur in the Ervay 3 biofacies and carbonate collections most frequently occur in the Franson 1 biofacies. By comparing the frequency and abundance of taxa in the Ervay 3 and Franson 1 biofacies, we can identify accessory taxa that may yield a more nuanced view of the intermingled association of chert and carbonate. In particular, chert collections from the Ervay 3 biofacies show limited input from brachiopod taxa that are frequent in carbonate collections of the Franson 1 biofacies (e.g., *Bathymyonia* and *Echinauris*). The brachiopods *Composita* and *Hustedia* stand out as being both more frequent and abundant compared with other brachiopod taxa in Ervay 3 versus Franson 1. The brachiopod "*Spiriferina*" and ramose bryozoans remain frequent in both chert and carbonate collections of Ervay 3 and Franson 1.

These results lead us to interpret that faunal communities existed along a gradient between carbonate and biosiliceous substrates in inner- to mid-ramp depositional environments (Fig. 10). This spectrum can be exemplified in two types of carbonate-chert community: carbonate with limited biosiliceous sediments (Franson 1 and Franson 2); and biosiliceous with limited carbonate sediments (Ervay 3). In both end-member communities, the brachiopod taxa *Bathymyonia*, *Echinauris*, *Derbyia*, and "*Spiriferina*," as well as ramose bryozoans, frequently occur and are typically common to abundant. Changes in the accessory brachiopod fauna characterize communities. In the primarily carbonate community, accessory taxa include the brachiopods *Neospirifer* and *Squamaria*. In the primarily biosiliceous community, accessory taxa include the brachiopods *Composita* and *Hustedia*. Bivalve and gastropod taxa occur infrequently and with rare abundance.

Conclusions

We conclude that the presence of biosiliceous deposition had little impact on community structure in strata of the Phosphoria Rock Complex. These results demonstrate that the faunal community was largely independent of its lithologic categorization as
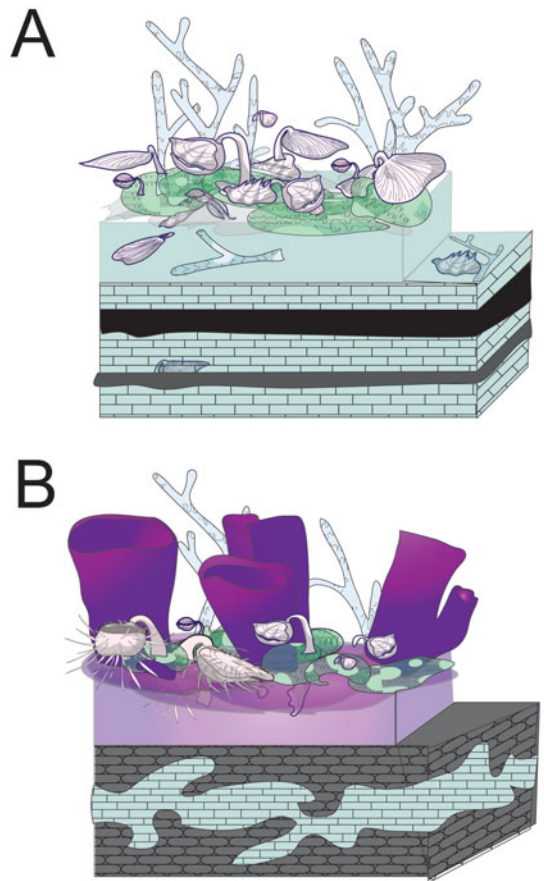

FIGURE 10. Faunal communities along a gradient between the carbonate and biosiliceous sedimentary environments. A, Carbonate community with limited biosiliceous sedimentary input. B, Biosiliceous community with limited carbonate sedimentary input.

either chert or carbonate. We document that lithology is only associated with minor changes in the frequency and abundance of accessory brachiopod taxa within the greater carbonate-chert community. We also conclude that biosiliceous sediments were primarily deposited in shallow-water settings of the inner- and mid-ramp facies, in agreement with previous studies.

Acknowledgments

Data Availability Statement

Data available from the Dryad Digital
Repository: https://doi.org/10.5061/dryad.
ngf1vhhwm.

Literature Cited

Beauchamp, B., and A. Baud. 2002. Growth and demise of Permian
    biogenic chert along northwest Pangea: evidence for end-Permian
    collapse of thermohaline circulation. Palaeogeography, Palaeo-
    climatology, Palaeoecology 184:37–68.
Beauchamp, B., and S. E. Grasby. 2012. Permian lysocline shoaling
    and ocean acidification along NW Pangea led to carbonate eradi-
    cation and chert expansion. Palaeogeography, Palaeoclimatology,
    Palaeoecology 15:73–90.
Behl, R. J. 2011. Chert spheroids of the Monterey Formation, Califor-
    nia (USA): early-diagenetic structures of bedded siliceous depos-
    its. Sedimentology 58:325–351.
Blakey, R. C. 2003. Carboniferous–Permian paleogeography of the
    assembly of Pangea. Pages 443–456 in T. E. Wong, ed. Proceed-
    ings of the XVth International Congress on Carboniferous and
    Permian Stratigraphy. Utrecht, Netherlands: Royal Netherlands
    Academy of Arts and Sciences:.
Blomeier, D., A. M. Dustira, H. Forke, and C. Scheibner. 2013. Facies
    analysis and depositional environments of a storm-dominated,
    temperate to cold, mixed siliceous-carbonate ramp: the Permian
    Kapp Starostin Formation in NE Svalbard. Norwegian Journal
    of Geology 93:75–93.
Bromley, R. G., and A. A. Ekdale. 1984. Trace fossil preservation
    in flint in the European Chalk. Journal of Paleontology
    58:298–311.
Butts, S. H., and D. E. G. Briggs. 2011. Silicification through time. In
    P. A. Allison and D. J. Bottjer, eds., Taphonomy: Process and Bias
    through Time. Topics in Geobiology 32:411–434.
Clapham, M. E. 2010. Faunal evidence for a cool boundary current
    and decoupled regional climate cooling in the Permian of western
    Laurentia. Palaeogeography, Palaeoclimatology, Palaeoecology
    298:348–359.
Clapham, M. E., and N. J. James. 2008. Paleoecology of early-middle
    Permian marine communities in eastern Australia: response to
    global climate change in the aftermath of the Late Paleozoic Ice
    Age. Palaios 23:748–750.
Cressman, E. R. 1955. Physical stratigraphy of the Phosphoria for-
    mation in part of southwestern Montana. U.S. Geological Survey
    Bulletin 1027-A:1–31.
Cressman, E. R., and R. W. Swanson. 1964. Stratigraphy and pet-
    rology of the Permian rocks of southwestern Montana. U.S. Geo-
    logical Survey Professional Paper 313-C:1–569.
Davydov, V. I., J. L. Crowley, M. D. Schmitz, and W. S. Snyder. 2018.
    New U-Pb constraints identify the end-Guadalupian and pos-
    sibly end-Lopingian extinction events conceivably preserved in

the passive margin of North America: implication for regional
    tectonics. Geological Magazine 155:119–131.
Dickinson, W. R. 2004. Evolution of the North American Cordillera.
    Annual Review of Earth and Planetary Science 32:13–45.
Gates, L. M., N. P. James, and B. Beauchamp. 2004. A glass ramp:
    shallow-water Permian spiculitic chert sedimentation, Sverdrup
    Basin, Artic Canada. Sedimentary Geology 168:125–147.
Finks, R. M., E. L. Yochelson, and R. P. Sheldon. 1961. Stratigraphic
    implications of a Permian sponge occurrence in the Park City For-
    mation of western Wyoming. Journal of Paleontology 35:564–568.
Hendrix, M. S., and C. W. Byers. 2000. Stratigraphy and sedimentology
    of Permian strata, Uinta Mountains, Utah: allostratigraphic controls
    on the accumulation of economic phosphate. In C. R. Glenn,
    L. Prévôt-Lucas, and J. Lucas, eds. Marine authigenesis: from global
    to microbial. SEPM Special Publication 66:349–367.
Hesse, R. 1989. Origin of chert: diagenesis of biogenic siliceous sedi-
    ments. Geoscience Canada 15:171–192.
Hiatt, E. E., and D. A. Budd. 2003. Extreme paleoceanographic con-
    ditions in a Paleozoic oceanic upwelling system: organic product-
    ivity and widespread phosphogenesis in the Permian Phosphoria
    Sea. In M. A. Chan and A. W. Archer, eds. Extreme depositional
    environments: mega end members in geologic time. Boulder,
    Colorado. Geological Society of America Special Papers 370:245–264.
Holland, S. M. 2005. The signatures of patches and gradients in
    ecological ordinations. Palaios 20:573–580.
Holland, S. M., and M. E. Patzkowsky. 2007. Gradient ecology of a
    biotic invasion: biofacies of the Type Cincinnatian series
    (Upper Ordovician), Cincinnati, Ohio Region, USA. Palaios
    22:392–407.
Holland S. M., A. I. Miller, D. L. Meyer, and B. F. Dattilo. 2001. The
    detection and importance of subtle biofacies within a single litho-
    facies: the Upper Ordovician Kope Formation of the Cincinnati,
    Ohio region. Palaios 16:205–217.
James, N. P. 1997. The cool-water carbonate depositional realm. In
    N. P. James and J. A. D. Clarke, eds. Cool-water carbonates.
    SEPM Special Publication 56:1–20.
Ketner, K. B. 2009. Mid-Permian Phosphoria Sea in Nevada and the
    upwelling model. U.S. Geological Survey Professional Paper
    1764:1–21.
Kidder, D. L., and D. H. Erwin. 2001. Secular distribution of bio-
    genic silica through the Phanerozoic: comparison of
    silica-replaced fossils and bedded cherts at the series level. Jour-
    nal of Geology 109:509–522.
Kidder, D. L., and I. Tomescu. 2016. Biogenic chert and the Ordovi-
    cian silica cycle. Palaeogeography, Palaeoclimatology, Palaeo-
    ecology 458:29–38.
Knauth, L. P. 1979. A model for the origin of chert in limestone.
    Geology 7:274–277.
Knauth, L. P. 1994. Petrogenesis of chert. In P. J. Heaney, C. T. Prewitt,
    and G. V. Gibbs, eds. Silica. Reviews in Mineralogy 29:233–256.
Maldonado, M., M. López-Acosta, C. Sitjà, M. García-Puig,
    C. Galobart, G. Ercilla, and A. Leynaert. 2019. Sponge skeletons
    as an important sink of silicon in the global oceans. Nature
    Geoscience 12:815–822.
Maliva, R. G., and R. Siever. 1989. Nodular chert formation in
    carbonate rocks. Journal of Geology 97:421–433.
Matheson, E. J., and T. D. Frank. 2020. An epeiric glass ramp:
    Permian low-latitude neritic siliceous sponge colonization and
    its novel preservation (Phosphoria Rock Complex). Sedimentary
    Geology 399:1–22.
McKelvey, V. E., J. S. Williams, R. P. Sheldon, E. R. Cressman, T.
    M. Cheney, and R. W. Swanson. 1959. The Phosphoria, Park
    City and Shedhorn Formations in the Western Phosphate Field.
    U.S. Geological Survey Professional Paper 313-A:1–47.
Miller, M. M. 1987. Dispersed remnants of a northeast Pacific
    fringing arc: Upper Paleozoic Terranes of Permian McCloud
    Faunal Affinity, western U.S. Tectonics 6:807–830.

Murchey, B. L. 2004. Regional analysis of spiculite faunas in the Permian Phosphoria Basin: implications for paleoceanography. *In* J. R. Hein, ed. Life cycle of the Phosphoria Formation: from deposition to post-mining environment. *In* M. Hale, ed. Handbook of Exploration and Environmental Geochemistry 8:111–135.

Murchey, B. L., and D. L. Jones. 1992. A mid-Permian chert event: widespread deposition of biogenic siliceous sediments in coastal, island arc and oceanic basins. Palaeogeography, Palaeoclimatology, Palaeoecology 96:161–74.

Patzkowsky, M. E., and S. M. Holland. 2012. Stratigraphic paleobiology: understanding the distribution of fossil taxa in time and space. University of Chicago Press, Chicago, p. 274.

Piper, D. Z., and P. K. Link. 2002. An upwelling model for the Phosphoria sea: a Permian, ocean-margin sea in the northwest United States. AAPG Bulletin 86:1217–1235.

Reid, C. M., N. P. James, B. Beauchamp, and T. K. Kyser. 2007. Faunal turnover and changing oceanography: late Palaeozoic warm-to-cool water carbonates, Sverdrup Basin, Canadian Arctic Archipelago. Palaeogeography, Palaeoclimatology, Palaeoecology 249:128–59.

Rigby, J. K., and D. W. Boyd. 2004. Sponges from the Park City Formation (Permian) of Wyoming. Journal of Paleontology 78:71–76.

Ritterbush, K. A. 2019. Sponge meadows and glass ramps: state shifts and regime change. Palaeogeography, Palaeoclimatology, Palaeoecology 513:116–131.

Rowden, A. A., K. Kröger, and M. R. Clark. 2015. Compositional patterns of benthic assemblages on the northwestern Ross Sea shelf, Antarctica: interacting environmental drivers operating at multiple spatial scales. Hydrobiologia 761:211–233.

Schoepfer, S. D., C. M. Henderson, G. H. Garrison, and P. D. Ward. 2012. Cessation of a productive coastal upwelling system in the Panthalassic Ocean at the Permian–Triassic Boundary. Palaeogeography, Palaeoclimatology, Palaeoecology 313–314:181–188.

Schoepfer, S. D., C. M. Henderson, G. H. Garrison, J. Foriel, P. D. Ward, D. Selby, J. C. Hower, T. J. Algeo, and Y. Shen. 2013. Termination of a continent-margin upwelling system at the Permian-Triassic boundary (Opal Creek, Alberta, Canada). Global and Planetary Change 105:21–35.

Schubert, J. K., D. L. Kidder, and D. H. Erwin. 1997. Silica-replaced fossils through the Phanerozoic. Geology 25:1031–1034.

Sheldon, R. P. 1963. Physical stratigraphy and mineral resources of Permian rocks in western Wyoming. U.S. Geological Survey Professional Paper 313-B:1–273.

Wardlaw, B. R. 1979. Studies of the Permian Phosphoria Formation and related rocks, Great Basin-Rocky Mountain Region. USGS Professional Paper 1163:1–38.

Wardlaw, B. R., and J. W. Collinson. 1986. Paleontology and deposition of the Phosphoria Formation. Contribution to Geology, University of Wyoming 24:107–142.

Whalen, M. T. 1996. Facies Architecture of the Permian Park City Formation, Utah and Wyoming: implications for the paleogeography and oceanographic setting of Western Pangea. *In* M. W. Longman and M. D. Sonnenfeld, eds. Paleozoic systems of the Rocky Mountain region. Rocky Mountain Section, SEPM (Society for Sedimentary Geology:355–378.

Wistort, Z. P., K. A. Ritterbush, and A. A. Ekdale. 2019. Trace fossils of problematic origin: assessing silicified trace fossils from the Permian of Utah, U.S.A. Palaios 34:631–638.

Wistort, Z. P., K. A. Ritterbush, and S. C. Hood. 2022. Cessation of a subtropical glass ramp during the Permian chert event: Murdock Mountain Formation, western U.S.A. Palaios 37:1–16.

Yochelson, E. L., and D. H. Van Sickle. 1968. Biostratigraphy of the Phosphoria, Park City, and Shedhorn Formations. U.S. Geological Survey Professional Paper 313-D:1–660.

Zharkov, M. A., and N. M. Chumakov. 2001. Paleogeography and sedimentation settings during Permian–Triassic reorganizations in biosphere. Stratigraphy and Geological Correlation 9:340–363.